The object of study is the recognition and identification of various objects in aerospace images. To solve the problems of compressing hyperspectral aerospace images with losses, the development of a compression algorithm is proposed. As a result, an algorithm has been developed for compressing aerospace images for subsequent recognition and identification of various objects using wavelet transform for processing high- and medium-resolution space images when monitoring from remote sensing satellites, based on the use of structural features of object images. In particular, orthogonal and wavelet transforms are presented, adapted for compression of hyperspectral aerospace images with losses, an adaptive discrete cosine transform algorithm is presented, followed by quantization with a loss level and compression. Thanks to a series of experiments on hyperspectral aerospace images, the effectiveness of the proposed algorithm in terms of the degree of compression, as well as the characteristics of the limits of its applicability, can be highlighted. The use of wavelets provides progressive compression of the bitstream, which makes it possible to achieve lossless compression with minimal loss of information due to the modified Huffman algorithm with a compression ratio of 9 more than 2.5 times in existing algorithms, as well as the quality metric of the restored images, the peak signal-to-noise ratio is sufficiently below 32.56.

The developed compression algorithm demonstrates the effectiveness of its application in terms of a set of characteristics and is superior to analogues. The scope and conditions for the practical use of the results obtained is a comparison of the proposed algorithm with the results of experiments obtained for universal compression algorithms for archivers and a compressor

Keywords: wavelet transform, Haar wavelet function, compression, hyperspectral aerospace images, compression algorithm, remote sensing

UDC 004.627

DOI: 10.15587/1729-4061.2024.306973

DEVELOPMENT OF AN ALGORITHM FOR COMPRESSING AEROSPACE IMAGES FOR THE SUBSEQUENT RECOGNITION AND IDENTIFICATION OF VARIOUS OBJECTS

Assiya Sarinova
PhD, Associate Professor*
Alexandr Neftissov
PhD, Associate Professor**
Leyla Rzayeva
PhD, Associate Professor*
Alimzhan Yessenov
PhD Candidate, Senior Lecturer*
Lalita Kirichenko
Doctoral Student**
Ilyas Kazambayev
Corresponding author
PhD Candidate, Junior Researcher**
E-mail: ilyaskazambayev@gmail.com
*Department of Intelligent Systems and Cybersecurity***
Research and Innovation Center "Industry 4.0"*
***Astana IT University
Mangilik El ave., 55/11, Business center EXPO, block C1,
Astana, Republic of Kazakhstan, 010000

Received date 02.04.2024
Accepted date 11.06.2024
Published date 28.06.2024

***How to Cite**: Sarinova, A., Neftissov, A., Rzayeva, L., Yessenov, A., Kirichenko, L., Kazambayev, I. (2024). Development of an algorithm for compressing aerospace images for the subsequent recognition and identification of various objects. Eastern-European Journal of Enterprise Technologies, 3 (2 (129)), 83–94. https://doi.org/10.15587/1729-4061.2024.306973*

1. Introduction

Currently, the development of software systems for image compression with data losses is an urgent research problem. Lossy data compression algorithms and methods cover a wide range, demonstrating high compression rates compared to lossless algorithms. Interest in digital imaging systems is driven by their ease of use and cost-effectiveness. However, their main disadvantage is their lower spatial resolution compared to traditional methods. Thus, details in the image may be less clear compared to images processed using traditional methods. In some cases, this can be critical, such as in medical diagnostics or scientific research where fine details are important.

In any image processing technique, the main challenge is to find an efficient representation to convey the image concisely. Modern theory and practice of signal processing, especially spectral analysis, uses special signals known as wavelets.

Discrete transforms are widely used in image compression due to their compact representation of information. These transforms can be classified into orthogonal transform types and algorithms, such as JPEG and SPIHT (Fig. 1).

The popularity of the use and application of wavelets in the field of image processing increased after the introduction of the concept of multiple-scale analysis by the French mathematician S. Mallat [1]. He was the first to use wavelets for image encoding. US scientists I. Daubechies and S. Mallat showed that the practical implementation of wavelet transforms is carried out using a two-band filter bank, known in the theory of subband coding (subband transforms). The theory of wavelet transforms arose at the beginning of the 20th century [2]. This includes the theory of the "Haar wavelet transform", which is a system of functions.

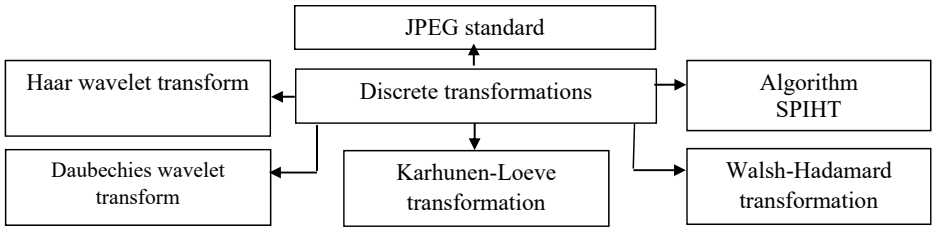

Fig. 1. Types of discrete transformations

With the development of technology and the growth of digital data volumes, the need for effective image compression methods is becoming increasingly urgent. The rapid increase in the number of digital images in various fields such as medicine, satellite imaging, computer vision and multimedia applications requires improved compression techniques to reduce the amount of information stored and transmitted without significant loss of quality. This makes research in the field of wavelet transforms and other data compression methods relevant and necessary for practical application. Nevertheless, current level of the wavelet transforms does not allow to reach the wanted accuracy leaving some details very fuzzy. On the other hand, all current algorithms and methods tend to reach the efficiency in compression in the way to not lose a lot of needed information.

Therefore, research devoted to the development of effective image compression methods, including wavelet transforms, is relevant and important for the further development of this field.

2. Literature review and problem statement

Currently, new methods and algorithms for encoding and decoding hyperspectral images (HSI) using wavelet transforms are being developed. For instance, research [3] demonstrate the importance of innovative approaches in the field of image processing. In particular, focuses on the development of a new hyperspectral imaging method that reduces cost and simplifies calibration, but has limitations in processing time and resolution. All this suggests that it is advisable to conduct a study on an integrated approach to processing remote sensing data with high accuracy is proposed, but it requires significant computing resources and high-quality source data. The advantage of the solutions are high precision of the hyperspectral images processing and disadvantage is the lack of information on accuracy and approbation of the methods.

In [4], a novel method termed Hyper-Laplacian Regularized Nonlocal Low-Rank Matrix Recovery (HyNLRMR) is presented for hyperspectral image (HSI) compressive sensing reconstruction. This method integrates nonlocal low-rank matrix recovery with a hyper-Laplacian prior to enhance the spatial and spectral structured sparsity of HSI data. The authors aim to address the limitations of conventional HSI compressive sensing reconstruction (CSR) techniques, particularly in preserving edges and suppressing artifacts. They employ the alternative direction multiplier method (ADMM) to optimize the proposed algorithm, and extensive experiments demonstrate its superiority over existing methods. On the other hand, the research does not demonstrate high accuracy of the solution due to its too universal application.

On the other hand, wavelet transform is one of the current trends in new compression algorithms for hyperspectral aerospace images (AI). The proposed satellite image compression system presents significant advancements in optimizing memory usage and achieving high compression performance while maintaining low complexity and high throughput [5]. However, there are several areas for improvement, particularly in scalability, real-time processing, error resilience, and long-term reliability. Addressing these limitations through future research and development will further enhance the system's applicability and effectiveness in satellite communication and image processing. The paper [6] proposes a novel approach to optimize memory usage for the Discrete Wavelet Transform (DWT) on Field-Programmable Gate Array (FPGA) devices and integrates it with an efficient image compression system for satellite images. Advantages of the research are a valuable contribution by addressing critical aspects of memory optimization and compression performance for satellite image processing on FPGA devices, the proposed method has clear practical implications for enhancing the efficiency of satellite image processing systems, potentially leading to better utilization of on-board resources and faster data transmission rates. Nevertheless, there is the need for further validation as the conclusions are primarily based on simulation and specific hardware evaluations. Additional validation through real-world testing and comparison with existing systems would strengthen the paper's claims. The paper [7] is significant for its innovative approach to improving compression efficiency while maintaining image quality, a critical challenge in remote sensing applications. The advantages of the solution lie in comprehensive evaluation, comparison with Existing Techniques demonstrating the accuracy. However, there are disadvantages as are primarily conducted on a specific set of hyperspectral images and does not discuss the generalizability of the results to other types of hyperspectral data or different remote sensing scenarios, which is crucial for broader applicability. In addition, there is lack of real-world validation as the experimental setup lacks real-world validation, such as tests on data collected from actual satellite missions or under varying environmental conditions, which would provide a more realistic assessment of the model's performance. The use of wavelets provides a progressive compressed bit stream, which allows achieving high compression rates (compression ratio – up to 6.6) due to intermediate and combined transformations. The advantage is achieved through the use of arithmetic coding. Disadvantages are: low compression performance; increasing the complexity of the algorithm in terms of the required RAM; relatively low quality with intermediate wavelet transforms. Number of bits per pixel BpP=0.7.

Researchers [8] investigated the compression of hyperspectral AI using the SPIHT algorithm. The standard SPIHT algorithm consists of three stages: initialization, sorting, and processing. The SPIHT algorithm generates three lists: a list of insignificant sets, a list of insignificant pixels, and a list of significant ones. The sorting and processing steps continue until the required number of bits are obtained. An indicator of the number of transformation levels of the SPIHT algorithm is the number to the right after the low-frequency and high-frequency coefficients – HL1, HL2 and HL3, meaning one-level (1D), two-level (2D) and three-level (3D) transformation. The reason for this is that at one of its stages a wavelet transform is applied. The Haar and Daubechies transformations are applied

to the image several times in a row. Regardless of the specific filter used, the image is decomposed into subbands so that the lower subranges correspond to the high frequencies of the image, and the upper ones correspond to the low frequencies of the image, in which the bulk of the image energy is concentrated. The advantages of the SPIHT algorithm include the ability to select the compression degree over a wide range – from 4 to 0.1 bits/pixel; no blockiness of the image at high compression rates; if part of the data is lost, it is possible to restore the entire image (with worse quality); the possibility that the resulting volume of data will have a strictly specified size. In this case, the problem that needs to be solved is the relative complexity of the implementation, instability to failures. Information transmitted before the failure allows to restore the image with worse quality, but information after the failure cannot be used.

Researchers [9] studied the compression of hyperspectral AIs using the 3D SPIHT algorithm. At the first stage, 3D DWT is used, at the second stage it is encoded with a 3D-SPIHT algorithm, where there is a significant correlation between different channel ranges. After decompression, the images are evaluated using PSNR=40, BpP=8.23. The 3D SPIHT algorithm provides a compression ratio of 1.92. Here is such a problem as the size of the image proportionally increases the time required to compress and restore the image, which increases the computational complexity of the algorithm.

Researchers considered [10] that one of the popular graphic formats designed for storing images is the JPEG algorithm, which allows lossless and lossy image compression. The algorithm of operation of a variation of the simplest lossy JPEG encoder consists of the following stages:

– preprocessing – preliminary processing of the image, leading it to a representation convenient for subsequent encoding;

– DCT is used by the JPEG encoder to transform an image from its spatial representation to its spectral representation;

– quantization is the stage at which the main loss of information occurs due to rounding of unimportant, high-frequency DCT coefficients;

– compression is the encoding of the received data using entropy algorithms (arithmetic coding, Huffman algorithm, etc.).

Based on the studies of hyperspectral aerospace images in the field of compression presented by scientists from China, the USA, India, and other countries, it can be inferred that existing lossless compression methods and algorithms for hyperspectral aerospace images can be enhanced by reducing their computational load and increasing the compression ratio through significant preprocessing steps. Additionally, new preprocessing stages, such as the Walsh-Hadamard transform in comparison with the discrete cosine transform, can be proposed to effectively increase the compression ratio and reduce the time required for forward and inverse transformations.

3. The aim and objectives of the study

The aim of the study is to develop an algorithm for compressing aerospace images for subsequent recognition and identification of various object. The achievement of this will allow to transmit the information with more efficiency on one hand and allow to increase the efficiency of the detection.

To achieve this aim, the following objectives are accomplished:

– mathematical formulation for compression algog rithm and prompt detection of changes in high- and medium-resolution space images at different times, based on the quantization of wavelet coefficients;

– analysis of the compression algorithm, based on the suitable wavelet function for analyzing real space images based on theoretical and practical research, carry out research of the developed algorithm using real space images.

4. Materials and methods

4. 1. Object and hypothesis of the study

The object of study is the recognition and identification of various objects in aerospace images. The hypothesis of the study is to achieve a significant increase in the compression ratio in comparison with analogues after wavelet transformations by modifying the adapted Huffman algorithm. Based on, analysis of other algorithms the compression rate for the suggested solution can achieve the rate of three four times.

For the mathematical formulation for compression algorithm and prompt detection of changes in high- and medium-resolution space images at different times, based on the quantization of wavelet coefficients the fundamental methods from vector calculus, signal processing, theory of information were applied.

For the analysis of the compression algorithm, based on the suitable wavelet function for analyzing real space images based on theoretical and practical research, carry out research of the developed algorithm using real space images a number of experiments were carried out using hyperspectral AI of the AVIRIS remote sensing system (Table 1) in the data format of the raster geographic information system IdrisiKilimanjaro. AVIRIS (Airborne Visible/Infrared Imaging Spectrometer) system – provides simultaneous acquisition of 224 spectral images with wavelengths ranging from 400 nm and 2500 nm. The proposed algorithm is also compared with the experimental results obtained for universal compression algorithms for WinRar, WinZip archivers and the Lossless/Lossy JPEG compressor, which uses an extension of the JPEG compression standard, widely used in remote sensing data processing systems. The experiments were performed on a PC with an IntelCore i5 2.5 GHz processor and 4 GB of RAM running the Windows 8.1 operating system.

Important parameters for the characteristics of hyperspectral images are the wavelength in nanometers and the spectral range.

Table 1

Main characteristics of hyperspectral remote sensing systems

Satellite system	Organization	Number of bands	Spectral range
Space sensor			
Hyperion, satellite EO-1	Goddard Space Flight Center	220	0.4–2.5 nm
AVIRIS (airborne visible infrared imaging spectrometer)	Jet Propulsion Laboratory	224	0.4–2.5 nm
Onboard sensor			
Resurs-P	JSC «Ross Cosmos «Progress»	128	0.4–1.1 nm

5. Results of research into aerospace image compression algorithms

5. 1. Mathematical formulation for compression algorithm and prompt detection of changes in high- and medium-resolution space images at different times

The research was carried out during the processing of high- and medium-resolution satellite images during monitoring from the Kazakh remote sensing satellites KazEOsat-1 and KazEOsat-2, based on the use of structural features of images of objects (Fig. 2).

a *b*

Fig. 2. Remote sensing: *a* — satellites KazEOsat-1 and KazEOsat-2, *b* — images [11]

Haar wavelet transform methods have a complete orthonormal system of basis functions with a local domain of definition [8]. These functions are called Haar wavelets, which are used in preprocessing in the image compression task. Wavelets are systems of functions used for information representation, filtering, compression and storage. The Haar wavelet is the following simple step function according to formula (1):

$$\Psi(x)=\begin{cases}1\left(0\le x<\frac{1}{2}\right),\\ -1\left(\frac{1}{2}\le x<1\right),\\ 0, \quad \text{in other cases.}\end{cases} \tag{1}$$

The Haar wavelet has a compact carrier. Obviously, the wavelet carrier combines two half-intervals $[0;1/2)\cup[1/2;1)$. The Haar wavelet is well localized in the time domain, but is not continuous (Fig. 3).

The Haar wavelet matrix has the property of orthogonality and looks as follows, formula (2):

$$H=\begin{pmatrix}\frac{1}{\sqrt{2}} & \frac{1}{\sqrt{2}}\\ \frac{1}{\sqrt{2}} & -\frac{1}{\sqrt{2}}\end{pmatrix}. \tag{2}$$

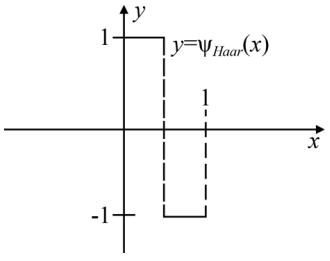

Fig. 3. Graph of the Haar wavelet function [1]

The use and application of wavelets in the field of image processing has increased in popularity since the introduction of the concept of multi-scale analysis. Wavelets are used here to encode images. The practical implementation of wavelet transforms is carried out using a two-band filter bank, known in the theory of subband coding (subband transforms). The main feature is the filter construction criteria. Based on the wavelet theory developed by Haar, the Daubechies family of wavelets is created.

The Daubechies Wavelet Transform method describes a family of wavelet transforms. Daubechies wavelet transforms combine the use of Haar wavelets and concepts such as weighted average and weighted difference. Based on this, two filters will be built for the Daubechies transformation – high-frequency and low-frequency, subject to quantization. Quantization is the process of reducing the amount of information required to store the original values of an image, with a partial loss of accuracy and quality. The final matrix is formed by dividing the original matrix by the quantization matrix. When restoring the original image, as in the previous example of the Haar wavelet, the resulting matrix is subject to transposition [12].

Transformation of a data structure based on the original hyperspectral AI storing the values of wavelet coefficients, using the example of a one-dimensional Haar wavelet. Fundamental to wavelet analysis is the idea of isolating information at different levels of detail. Details, in turn, can be thought of as scale or resolution information. The idea on which the application of wavelet analysis to image compression is based: isolating the information that details carry and removing those information details that are small and have little effect on the image as a whole.

Proposed stages of the algorithm using Haar wavelets for compression of hyperspectral aerospace images:

1. Transformation of the data structure based on the original hyperspectral AI, storing the values of the wavelet coefficients, using the example of a one-dimensional Haar wavelet.

2. Transformation of the data structure based on the original hyperspectral AI, storing the values of the wavelet coefficients, using the example of a two-dimensional Haar wavelet.

3. Transformation of the obtained data structures based on steps 1–2 by quantization of the wavelet coefficients.

4. Using standard criteria for the quality of restored images.

5. Compression of the obtained structures of stage 4 by the modified Huffman algorithm.

The Haar function system has the main properties specific to wavelets: local domain of definition (limited by carriers), orthogonality and unit norm, zero mean. Currently, many researchers, especially those working in practical applications for image compression, understand wavelets as a broader class of functions.

The functions proposed by the Hungarian mathematician A. Haar in 1910 and subsequently called Haar wavelets are discontinuous and very convenient for initial image analysis. The Haar function is defined by the formula:

$$\Psi(t)=\begin{cases}1 \text{ if } t\in[0,1/2),\\ -1 \text{ if } t\in[1/2,1),\\ 0 \text{ if } t\notin[0,1).\end{cases}$$

Haar wavelet transform:

– the transformation method is that the image lines are transformed, thereby carrying out a one-dimensional wavelet transform;

– finding half-sums and half-differences using Haar wavelets, as the use of low and high-frequency filters [9].

Considering the details of the stages of converting hyperspectral AI channel values $I[m, n, k]$ based on one-dimensional Haar wavelet using existing low-pass and high-pass coefficient function filters.

Step 1. Creation of a sequence based on the original image with the following function:

$$f\left(I[m,n,k]\right)=I[m+1,n+1,k-1]_1\times\varphi_{n.0}\left(I[m,n,k]\right)+\ldots$$
$$\ldots+I[m+1,n+1,k-1]_{2^n}\times\varphi_{n,2^{n-1}}\left(I[m,n,k]\right),$$

where n – serial number of the term.

Step 2. Calculation of the average values of pairwise adjacent values using the following formulas:

– half sums:

$$a_{I[m,n,k-1]}=\frac{I[m+1,n+1]+I[m+2,n+2]}{2};\qquad(3)$$

– semi-differences:

$$d_{I[m,n,k-1]}=\frac{I[m+1,n+1]-I[m+2,n+2]}{2}.\qquad(4)$$

Step 3. Obtaining new data structures for hyperspectral AI $a_{I[m,n,k-1]}$ and $d_{I[m,n,k-1]}$ based on half sums and differences.

Step 4. Decomposition of $f(t)$ based on step 2 and 3, half-sum and half-difference components:

$$f\left(I[m,n,k]\right)=a_{I[m,n,k-1],0}\times\varphi_{I[m,n,k-1],0}\left(I[m,n,k]\right)+\ldots$$
$$\ldots+a_{I[m,n,k-1],2^{n-1}}\times\varphi_{I[m,n,k-1],2^{n-1}-1}\left(I[m,n,k]\right)+$$
$$+d_{I[m,n,k-1],0}\times\psi_{I[m,n,k-1],0}\left(I[m,n,k]\right)+\ldots$$
$$\ldots+d_{I[m,n,k-1],2^{n-1}-1}\times\psi_{I[m,n,k-1],2^{n-1}-1}\left(I[m,n,k]\right).\qquad(5)$$

Step 5. Calculation of wavelet coefficients: low frequency:

$$a_{I[m,n,k-1],n}=\frac{I[m+1,n+1]_{n+1}+I[m+2,n+2]_{n+2}}{\sqrt{2}},$$

$$n=0,\ldots 2^{n-1}-1,\qquad(6)$$

using the properties of orthogonality and normalization of the function $f(I[m, n, k])$, calculate high-frequency coefficients $d_{I[m,n,k],n}$ according to the following formula [10]:

$$d_{I[m,n,k-1],j}=\frac{I[m+1,n+1]_{j+1}-I[m+2,n+2]_{j+2}}{\sqrt{2}},\qquad(7)$$

where $j=0,\ldots 2^{n-1}-1$.

Let's place the result in matrices $I^{\Psi}_{Haar\,I}[m,n,k]$.

After the Haar wavelet transformation, let's obtain the wavelet coefficients of two components – low-frequency and high-frequency. If it is necessary to compress this image, it is possible to pay attention to the value of the high-frequency coefficients, which may be subject to the quantization procedure. Let's remember only the specified % of the largest coefficients (low-frequency), the remaining smallest (%) coefficients are set to zero (high-frequency).

At the stage of restoring the original image channels, the spectral components are decoded by transforming the matrix of Haar wavelet coefficients.

The advantage of conversion: the ability to highlight low-frequency areas in the image while maintaining excellent quality, due to which the compression ratio is increased.

Based on the proposed schemes and developed effective algorithms for lossless hyperspectral AI compression in p. p. 2. 1 it is possible to conclude that the requirements for ensuring high compression ratios and computational efficiency are met [13].

One way to obtain a two-dimensional wavelet transform of an image of size $2^m\times2^n$, is to first apply a one-dimensional wavelet transform to each of the rows 2^m of hyperspectral AI channels, and then apply a one-dimensional wavelet transform to each of the 2^n columns.

The first way is to have the image rows converted first and then transform the image columns with the converted rows.

Considering the details of the stages of converting hyperspectral AI channel values $I[m, n, k]$ based on two-dimensional Haar wavelet.

Step 1. Creation a sequence based on the original image with the following function:

$$f\left(I[m,n,k],I'[m,n,k]\right)=$$
$$=\sum_{i=1}^{I[m,n,k]}\sum_{j=1}^{I[m,n,k]}I[m,n,k]_{i,j}\,I[m,n,k]_{I_i\times I_j}\times$$
$$\times\left(I[m,n,k],I'[m,n,k]\right).\qquad(8)$$

where:

$$I_i\times I_j\equiv\left[\frac{i-1}{m},\frac{i}{n}\right)\times\left[\frac{j-1}{m},\frac{j}{n}\right)=$$
$$=\left(I[m,n,k],I'[m,n,k]\right):I[m,n,k]\in\left[\frac{i-1}{m},\frac{i}{n}\right).\qquad(9)$$

and:

$$I'[m,n,k]\in\left[\frac{j-1}{m},\frac{j}{n}\right),\qquad(10)$$

$$X_{I_i\times I_j}\left(I[m,n,k],I'[m,n,k]\right)=$$
$$=\begin{cases}1 \text{ if } I[m,n,k],I'[m,n,k],\\ 0 \text{ otherwise}\end{cases}=$$
$$X_{I_j}\left(I[m,n,k]X_{I_j}I'[m,n,k]\right)=$$
$$=\phi_{2,i-1}\left(I[m,n,k]\right)\phi_{2,j-1}\left(I'[m,n,k]\right).\qquad(11)$$

Step 2. Based on the generated function, let's transform the image lines to obtain wavelet coefficients:

$$f\left(I[m,n,k],I'[m,n,k]\right)=$$
$$=\sum_{i=1}^{4}\sum_{j=1}^{4}I[m,n,k]_{i,j-1}\,\phi_{2,j-1}\left(I[m,n,k]\right)\times$$
$$\times\phi_{2,i-1}\left(I'[m,n,k]\right)=$$
$$=\sum_{i-1}^{4}\left\{\sum_{j-1}^{4}x_{i,j}\,\phi_{2,i-1}\left(I'[m,n,k]\right)\right\}\phi_{2,i-1}\left(I[m,n,k]\right)=$$
$$=\sum_{i=1}^{4}I\left[\widetilde{m,n,k}\right]_{l}\left(I'[m,n,k]\right)\phi_{2,i-1}\left(I[m,n,k]\right), \quad (12)$$

where:

$$I\left[\widetilde{m,n,k}\right]_{l}\left(I'[m,n,k]\right)=$$
$$=\sum_{j=1}^{4}I[m,n,k]_{i,j}\,\phi_{2,j-1}\left(I'[m,n,k]\right). \quad (13)$$

As a result, let's receive a new set with coefficients resulting from the wavelet transform $I[m, n, k]$:

$$I\left[\widetilde{m,n,k}\right]\left(I'[m,n,k]\right)=$$
$$=a_{0,0}^{i}\,\phi_{0,0}\left(I'[m,n,k]\right)+d_{0,0}^{i}\,\psi_{0,0}\left(I[m,n,k]\right)+\ldots$$
$$\ldots+d_{1,0}^{i}\,\psi_{1,0}\left(I[m,n,k]\right)+d_{1,1}^{i}\,\psi_{1,1}\left(I[m,n,k]\right). \quad (14)$$

Step 3. Based on the generated rows with coefficients, let's transform the image columns:

$$f(I[m,n,k],I'[m,n,k])=$$
$$\left\{\sum_{i=1}^{m}a_{0,0}^{i}\,\phi_{2,i-1}\left(I[m,n,k]\right)\right\}\phi_{0,0}\left(I'[m,n,k]\right)+$$
$$+\left\{\sum_{i=1}^{m}d_{0,0}^{i}\,\phi_{2,i=j}\left(I[m,n,k]\right)\right\}\psi_{0,0}\left(I'[m,n,k]\right)+\ldots$$
$$\ldots+\left\{\sum_{i=1}^{n}d_{1,0}^{n}\,\phi_{1,0}\left(I[m,n,k]\right)\right\}\psi_{1,0}\left(I'[m,n,k]\right)+$$
$$+\left\{\sum_{i=1}^{n}d_{1,1}^{n}\,\phi_{2,i-1}\left(I[m,n,k]\right)\right\}\psi_{1,1}\left(I'[m,n,k]\right).$$

The results placed in $I_{Haar\ II}^{\Psi}[m,n,k]$.

So, one of the ways to obtain a two-dimensional wavelet transform of an image of size $m\times n$, is to first apply a one-dimensional wavelet transform to each of the m rows, and then apply a one-dimensional wavelet transform to each of the n columns.

For example of a fragment of a hyperspectral AI [14]:

$$I[m,n,k]=\begin{pmatrix}128 & 123 & 0 & 105\\ 0 & 105 & 0 & 105\\ 128 & 121 & 128 & 121\\ 0 & 103 & 128 & 121\end{pmatrix}.$$

By applying the one-dimensional Haar wavelet transform to the first row, the values of the approximation coefficients and differences are calculated:

$$\begin{cases}a_1=\dfrac{128+0}{\sqrt{2}};\\ a_1=\dfrac{123+105}{\sqrt{2}};\\ d_1=\dfrac{128-0}{\sqrt{2}};\\ d_1=\dfrac{123-105}{\sqrt{2}}.\end{cases}$$

Similarly, the one-dimensional Haar wavelet transform is applied to the remaining rows of the matrix $I[m, n, k]$. The result is a new matrix, the first two columns of which contain the values of the approximation coefficients of each row, and the next two columns contain the values of the difference coefficients.

The result is a transformed first-level matrix:

$$I[m,n,k]=\begin{pmatrix}64 & 114 & 0 & 0\\ 64 & 112 & 0 & 0\\ -64 & -9 & 0 & 0\\ -64 & -9 & 0 & 0\end{pmatrix}.$$

The converted matrix is divided into four second-level filters.

From Fig. 4 it is clear that a full quarter of the two-dimensional transformation coefficients are the result of the action of a high-pass filter *(H)* on the rows, and then its action on the resulting columns of information. This is the block of coefficients in the lower right corner of the diagram, labeled *HH* [15].

$LL=\begin{pmatrix}64 & 114\\ 64 & 112\end{pmatrix}$	$LH=\begin{pmatrix}0 & 0\\ 0 & 0\end{pmatrix}$
$HL=\begin{pmatrix}-64 & -9\\ -64 & -9\end{pmatrix}$	$HH=\begin{pmatrix}0 & 0\\ 0 & 0\end{pmatrix}$

Fig. 4. *LL, HL, LH, HH* Filter Matrix (developed by the authors)

The other quarter of the two-dimensional transform coefficients is the result of the low-pass filter (*L*) acting on the columns of information that have already been passed through the high-pass filter. This block, designated *LH*, is located in the upper right corner of Fig. 1. Similarly, the *HL* block located in the lower left corner is the result of low-frequency processing of the rows, followed by high-frequency processing of the columns [16].

Currently, new methods and algorithms for encoding and decoding hyperspectral AIs using wavelet transforms are being developed [17–23]. For example, a group of researchers Emmanuel, Sujithra, Pizzolante believe that wavelet transform [24, 25] is one of the current trends in new compression algorithms for hyperspectral AI. The use of wavelets provides a progressive compressed bit stream, which allows achieving high compression rates (compression ratio – up to 6.6) due to intermediate and combined transformations. The advantage is achieved through the use of arithmetic coding. Disadvantages are: low compression performance; increasing the complexity of the algorithm in terms of the required RAM; relatively low quality with intermediate wavelet transforms.

In the above-described wavelet transformations, hyperspectral AI channels were divided into two filters: low frequency (LF) and high frequency (HF). Haar wavelets (one-dimensional and two-dimensional transformation) and Daubechies wavelet were used as filters.

After wavelet transformations, the high-frequency components of hyperspectral AI are subject to quantization (rounding) or values close to 0 – zeroing, which is subsequently encoded. The effectiveness of using the wavelet transform is that the Haar and Daubechies wavelets are preparatory data processing to present a more compact rep-

resentation of the data and subsequent compression. The loss level is controlled by the quantization step.

Step 1. Based on the original image and the found low-pass and high-pass filters, linear quantization matrices are calculated for one-dimensional Haar wavelet, two-dimensional Haar and Daubechies:

$$\begin{cases} I^{\Psi}_{Haar\ I}[m,n,k]=\dfrac{I[m,n,k]}{h}; \\ I^{\Psi}_{Haar\ II}[m,n,k]=\dfrac{I[m,n,k]}{h}; \\ I^{\Psi}_{Db}[m,n,k]=\dfrac{I[m,n,k]}{h}, \end{cases} \quad (15)$$

where h –the quantization step.

The result is saved in matrices:

$$I'^{\Psi}_{Haar\ I}[m,n,k]=\frac{I'[m,n,k]}{h}. \quad (16)$$

Step 2. Based on quantized matrices (15) let's form the converted images. The result is saved in matrices $I^{\Psi}_{Haar\ I}[m,n,k]$.

5. 2. Analysis of the compression algorithm, based on the suitable wavelet function

Based on the analysis, it shows that despite significant advances in the field of hyperspectral image compression, unresolved issues remain related to computational complexity and processing time. The solution is in developing new preprocessing and compression algorithms that enhance the efficiency of compression and image reconstruction processes.

At this stage, based on the obtained transformations, the converted hyperspectral AI channels were compressed by a modified Huffman algorithm.

The task of entropy coding is to convert a field of code values (obtained after conversion and quantization into integers) into a bit stream and back.

The well-known standard table of Huffman codes is recommended for JPEG images, not for hyperspectral AI, therefore a generated "intuitive-software" table is proposed for coding, Table 2.

The Table 2 modification is as follows:

1) assign each possible pair *RZ* a natural number (intMerge; starting from two, these numbers are indicated in parentheses in the table). As it is possible to see from the Table 2, in one row they decrease with increasing *R*, and in one column they increase with *Z*;

2) consider the binary notation of the number intMerge and pay attention to its length (lenMerge). For example, for (*R*; *Z*)=(4;7) intMerge=117, binary notation –1110101, lenMerge=7;

3) build the code as follows: take one (lenMerge–1) times, assign 0 and the binary representation of the number intMerge without the leading one. For clarity, after the zero it is possible to add an apostrophe: 1111110'110101.

For example from the Table 1: (*R*;*Z*)=(14;1) intMerge=17, binary notation – 10001, lenMerge=5. Huffman code: 11110'0001.

The number *Z* does not exceed 14, since it is possible to replace the sequence of 15 zeros with the code 11111110'00000000 (as if intMerge were equal to 256). The code for the end of the block is 00. The pair (*R*;*Z*)=(15;0) is coded as 01. If *R* exceeds 16, then it is possible to assign intMerge, starting from 257, similarly.

This modification made it possible to increase the degree of compression of hyperspectral AIs due to the analysis of the frequencies of *R* and *Z* pairs, since codes of shorter length are allocated to more common values.

In result, the graphs and images were obtained are shown below in Fig. 5–7.

The comparison demonstrates achieved results in compression of the images.

The obtained results are demonstrated in Table 3.

The results obtained demonstrate the achieved accuracy of the proposed method using Haar wavelets, quantization of coefficients and compression by a modified Huffman algorithm, Fig. 8–10.

Table 2

"Intuitive-software" table of Huffman codes

	R				
Z	1	2	3	4	5
	6	7	8	9	10
	11	12	13	14	15
Z=0	1110'111 (15)	1110'110 (14)	1110'101 (13)	1110'100 (12)	1110'011 (11)
	1110'010 (10)	1110'001 (9)	1110'000 (8)	110'11 (7)	110'10 (6)
	110'01 (5)	110'00 (4)	10'1 (3)	10'0 (2)	01
Z=1	11110'1110 (30)	11110'1101 (29)	11110'1100 (28)	11110'1011 (27)	11110'1010
	11110'1001	11110'1000	11110'0111	11110'0110	11110'0101
	11110'0100	11110'0011	11110'0010 (18)	11110'0001 (17)	11110'0000 (16)
Z=2	111110'01101 (45)	111110'01100 (44)	111110'01011	111110'01010	111110'01001
	111110'01000	111110'00111	111110'00110	111110'00101	111110'00100
	111110'00011	111110'00010	111110'00001	111110'00000 (32)	11110'1111 (31)
...	...	...	...	...	...
Z=14	11111110'1111111 (255)	...	...	...	(...etc.)

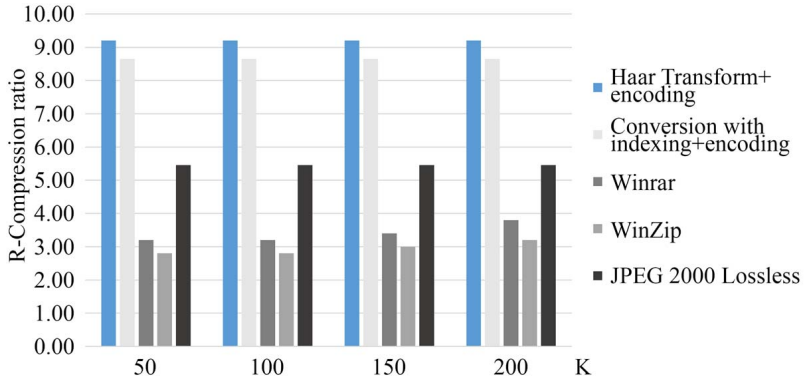

Fig. 5. Comparison of lossless compression algorithms by compression ratio (developed by the authors)

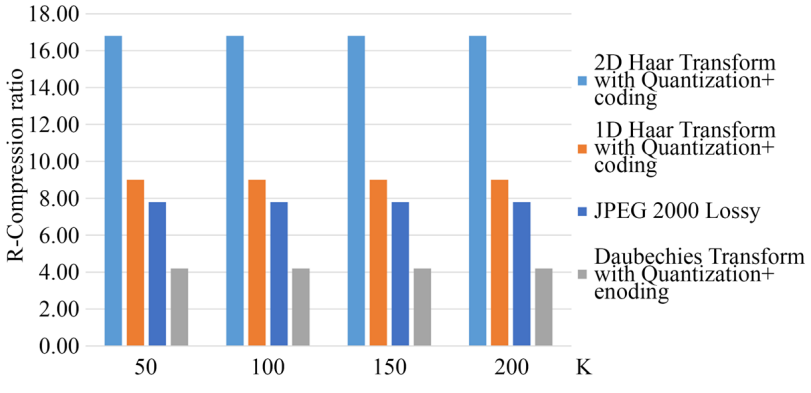

Fig. 6. Indicators of compression rates of lossy algorithms (developed by the authors)

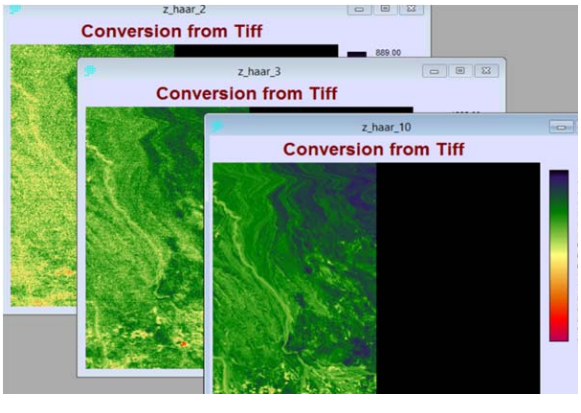

a

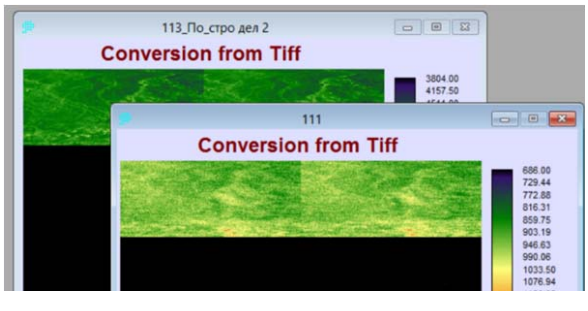

b

Fig. 7. Haar wavelet transform: *a* — one dimensional; *b* — two dimensional (developed by the authors)

Table 3

Characteristics of test hyperspectral AIs by number of channels

Number of channels	Size Images	Size (byte)	Number of channels	Size Images	Size (byte)
100	50*50	1081600	200	50*50	2163200
100	100*100	4080400	200	100*100	8160800
100	200*200	16160400	200	200*200	32320800
100	300*300	36240400	200	300*300	72480800
100	400*400	64320400	200	400*400	128640800
100	614*512	125747200	200	614*512	251494400
150	50*50	1622400	224	50*50	2421632
150	100*100	6120600	224	100*100	9140096
150	200*200	24240600	224	200*200	36199296
150	300*300	54360600	224	300*300	81178496
150	400*400	96480600	224	400*400	144077696
150	614*512	188620800	224	614*512	281673728

The advantage of the two-dimensional Haar wavelet transform with losses: the ability to identify low-frequency regions of the image, which are subsequently effectively compressed by entropy algorithms due to its division into levels. But at the same *time*, the main disadvantage of the conversion remains: the quality of the reconstructed images drops sharply as the quantization rate increases. In future research, this disadvantage will be eliminated by reducing the computational complexity of compression.

0	400	227	138	0	352	220	138	0	384	206	138
0	48	5	0	0	0	18	0	0	64	24	0
0	160	221	138	0	432	211	138	0	176	196	138
0	128	13	0	0	16	19	0	0	48	14	0
0	208	208	138	0	80	193	138	0	224	181	138
0	-176	18	0	0	-80	9	0	0	192	11	0
0	112	201	138	0	240	186	138	0	400	192	138
0	-80	1	0	0	-176	0	0	0	-48	22	0
0	336	188	138	0	144	187	138	0	368	200	138
0	80	-2	0	0	-144	11	0	0	-48	30	0
0	368	192	138	0	272	191	138	0	400	205	138
0	80	16	0	0	-112	7	0	0	-48	31	0
0	192	207	138	0	320	211	138	0	256	212	138
0	192	29	0	0	0	19	0	0	-128	32	0
0	360	214	138	0	240	206	138	0	160	188	138
0	136	46	0	0	16	38	0	0	-32	24	0

Fig. 8. Two-dimensional Haar transform with low-frequency and high-frequency coefficients (developed by the authors)

0	200	114	69	0	176	110	69	0	192
0	24	3	0	0	0	9	0	0	32
0	80	111	69	0	216	106	69	0	88
0	64	7	0	0	8	10	0	0	24
0	104	104	69	0	40	97	69	0	112
0	0	9	0	0	0	5	0	0	96
0	56	101	69	0	120	93	69	0	200
0	0	0	0	0	0	0	0	0	0
0	168	94	69	0	72	94	69	0	184
0	40	0	0	0	0	6	0	0	0
0	184	96	69	0	136	96	69	0	200
0	40	8	0	0	0	4	0	0	0
0	96	104	69	0	160	106	69	0	128
0	96	15	0	0	0	10	0	0	0
0	180	107	69	0	120	103	69	0	80
0	68	23	0	0	8	19	0	0	0
0	112	103	69	0	88	96	69	0	184

Fig. 9. Quantization stage with step 1 with compression ratio of 6.7 (developed by the authors)

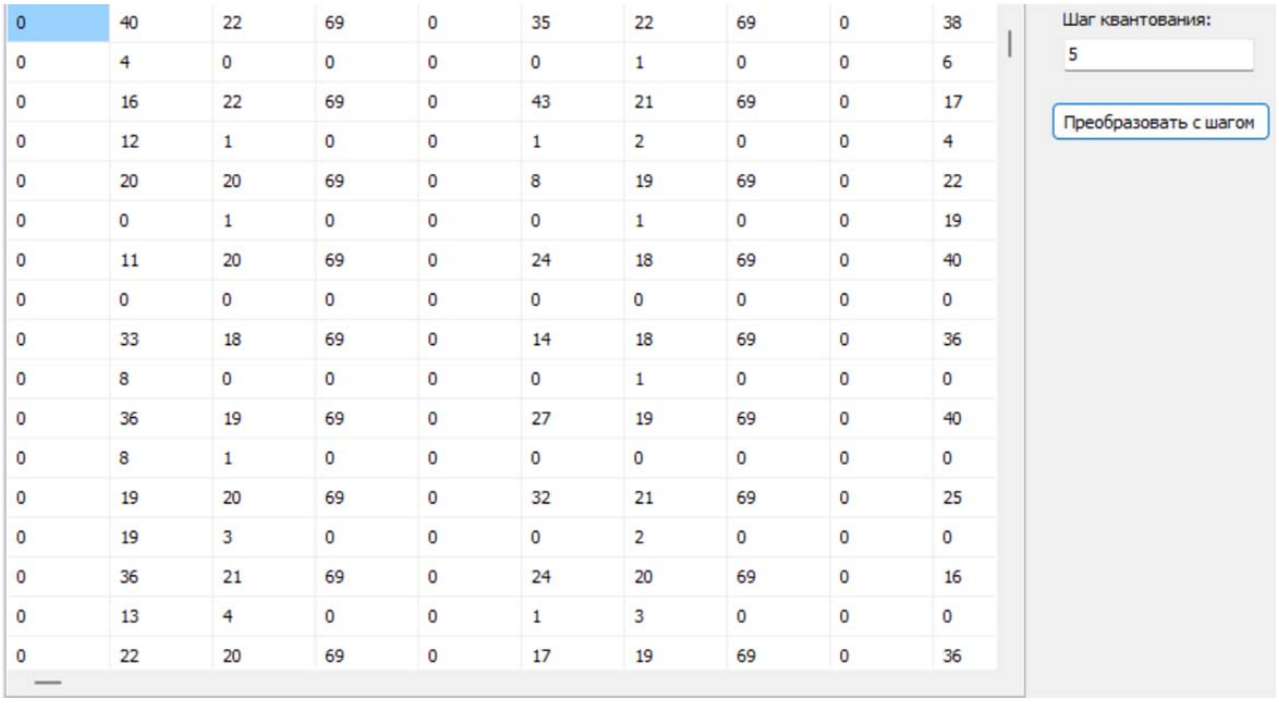

0	40	22	69	0	35	22	69	0	38
0	4	0	0	0	0	1	0	0	6
0	16	22	69	0	43	21	69	0	17
0	12	1	0	0	1	2	0	0	4
0	20	20	69	0	8	19	69	0	22
0	0	1	0	0	0	1	0	0	19
0	11	20	69	0	24	18	69	0	40
0	0	0	0	0	0	0	0	0	0
0	33	18	69	0	14	18	69	0	36
0	8	0	0	0	0	1	0	0	0
0	36	19	69	0	27	19	69	0	40
0	8	1	0	0	0	0	0	0	0
0	19	20	69	0	32	21	69	0	25
0	19	3	0	0	0	2	0	0	0
0	36	21	69	0	24	20	69	0	16
0	13	4	0	0	1	3	0	0	0
0	22	20	69	0	17	19	69	0	36

Fig. 10. Quantization stage in steps of 5 with compression ratio of 9,2. (developed by the authors)

6. Discussion of the results of an experiment on an algorithm for compressing aerospace images

Experiments for the compression algorithm considering inter-channel correlation and Haar wavelet processing show the following interesting factors that were obtained through equations (12)–(14). Considering the results of preparatory processing experiments based on wavelet and orthogonal transformations before lossless hyperspectral AI compression.

Possible following stages of preparatory processing of hyperspectral AI based on the proposed stages:

– transformation of a data structure based on the original hyperspectral AI, storing the values of wavelet coefficients, using the example of one-dimensional and two-dimensional Haar wavelets;

– indexed data structure transformation based on the original hyperspectral AI.

To determine the effectiveness of the proposed algorithm in terms of the degree of compression, as well as the limits of its applicability, a number of experiments were carried out on hyperspectral AIs. The proposed algorithm is compared with the experimental results obtained for universal compression algorithms for archivers and the Lossles JPEG 2000 compressor, widely used in remote sensing data processing systems. Experiments on the compression ratio in comparison with well-known archivers and JPEG 2000 are presented in the graph by lossless compression ratio. Preparatory processing and compression algorithms.

As can be seen from Fig. 5, the degree of preparatory processing and compression exceeds the WinRar, WinZip and Losless JPEG archivers by more than 80 %.

Experiments based on two-dimensional Haar and Daubechies wavelets show the following interesting factors. The compression ratios of the Haar, Daubechies and JPEG 2000 Lossy wavelet transforms are presented in Fig. 6. The compression ratios of the one-dimensional and two-dimensional Haar wavelet transforms with losses are superior in the compression ratio to the Daubechies wavelet of the JPEG Lossy compressor.

Examples of one-dimensional and two-dimensional Haar wavelet transforms, Fig. 7, a, *b*, *K*=2, 3, 10.

In order to increase the computational efficiency and degree of compression of hyperspectral AI, various variants of algorithm experiments have been proposed.

In comparison based on Fig. 8–10, it can be noted that the compression rate from step 1 to step 5 increases from 6.7 to 9.2.

The main limitations of the research are the need of the bigger database, to provide more information of the accuracy, the amount of the hyperspectral images from the satellite is also limited and can be acquired through time.

The disadvantage of the research is the requirement of high power computing systems to do the compression, which in return balanced by high accuracy.

In the future research the work will be aimed at lowering the required amount of computing resources.

Within the framework of the conducted research and the developed Haar wavelet transformation algorithm, all the data on satellite systems that are important are presented above, the physical component of hyperspectral images does not affect the compression result. Taking into account physical characteristics is beyond the scope of this study, but in the future it will be taken into account in further studies, since this is another task of transformations before compression.

7. Conclusions

1. An algorithm has been developed based on Haar wavelet transforms with modification and adaptation of Huffman codes, which allows increasing the compression ratio of hyperspectral images to 9.2, which is higher than analogues due to quantization of high-frequency coefficients of reconstructed images. Thanks to the pre-processing of 2D

Haar wavelet representations of hyperspectral images, which achieves high compression ratios compared to existing studies.

2. An approach to compression of hyperspectral images with losses was developed, defined in adaptive and difference transforms based on wavelet transforms, an adapted quantization table, and the PSNR quality metrics criterion lies in a fairly average range of 30–50 %, in which the percentage of quality of the reconstructed images is preserved up to 85–90 %. The result is achieved thanks to the quantization table and its parameters, where the quantization coefficient is 5. This means rounding the values of the original image after wavelet transformations to a loss level of only 5 %.

In addition, the results of comparison of the wavelet transform of a hyperspectral image using the obtained quantization coefficients were developed and obtained, which indicate the effectiveness of adaptive Huffman coding. This modification improves the compression ratio of hyperspectral images by analyzing the frequencies of channel pairs, since shorter code lengths are assigned more common values and allow bits to be stored in a reduced size.

Conflict of interest

The authors declare that they have no conflict of interest in relation to this research, whether financial, personal, authorship or otherwise, that could affect the research and its results presented in this paper.

Financing

The article was written within the state order for the implementation of the scientific pro-gram under the budget program of the Republic of Kazakhstan 217 "Development of Science", subprogram 101 "Program-targeted funding of the scientific and/or technical activity at the expense of the national budget" on the theme: "Development of technology for intelligent preprocessing of aerospace images for recognition and identification of various objects" Grant IRN AP19678773.

Data availability

Data will be made available on reasonable request.

Use of artificial intelligence

The authors confirm that they did not use artificial intelligence technologies when creating the current work.

References

1. Mallat, S. (1999). A Wavelet Tour of Signal Processing. Academic Press. https://doi.org/10.1016/b978-0-12-466606-1.x5000-4
2. Salomon, D. (2007). Data compression: The complete reference. Springer, 1092.
3. Ceamanos, X., Valero, S. (2016). Processing Hyperspectral Images. Optical Remote Sensing of Land Surface, 163–200. https://doi.org/10.1016/b978-1-78548-102-4.50004-1
4. Xue, J., Zhao, Y., Liao, W., Chan, J. C.-W. (2019). Hyper-Laplacian regularized nonlocal low-rank matrix recovery for hyperspectral image compressive sensing reconstruction. Information Sciences, 501, 406–420. https://doi.org/10.1016/j.ins.2019.06.012
5. Prabhakar, T. V. N., Geetha, P. (2017). Two-dimensional empirical wavelet transform based supervised hyperspectral image classification. ISPRS Journal of Photogrammetry and Remote Sensing, 133, 37–45. https://doi.org/10.1016/j.isprsjprs.2017.09.003
6. Pranitha, K., Kavya, G. (2023). An efficient image compression architecture based on optimized 9/7 wavelet transform with hybrid post processing and entropy encoder module. Microprocessors and Microsystems, 98, 104821. https://doi.org/10.1016/j.micpro.2023.104821
7. Shi, C., Zhang, J., Zhang, Y. (2016). Content-based onboard compression for remote sensing images. Neurocomputing, 191, 330–340. https://doi.org/10.1016/j.neucom.2016.01.048
8. Puri, A., Sharifahmadian, E., Latifi, S. (2014). A Comparison of Hyperspectral Image Compression Methods. International Journal of Computer and Electrical Engineering, 6 (6), 493–500. https://doi.org/10.17706/ijcee.2014.v6.867
9. Lin, H.-C., Hwang, Y.-T. (2011). Lossless Compression of Hyperspectral Images Using Adaptive Prediction and Backward Search Schemes. Journal of Information Science and Engineering, 27, 419–435. Available at: https://www.researchgate.net/publication/220588090_Lossless_Compression_of_Hyperspectral_Images_Using_Adaptive_Prediction_and_Backward_Search_Schemes
10. Mora Pascual, J., Mora Mora, H., Fuster Guilló, A., Azorín López, J. (2015). Adjustable compression method for still JPEG images. Signal Processing: Image Communication, 32, 16–32. https://doi.org/10.1016/j.image.2015.01.004
11. KazEOSat-1. Available at: https://www.eoportal.org/satellite-missions/kazeosat-1
12. Nian, Y., He, M., Wan, J. (2015). Lossless and near-lossless compression of hyperspectral images based on distributed source coding. Journal of Visual Communication and Image Representation, 28, 113–119. https://doi.org/10.1016/j.jvcir.2014.06.008
13. Cheng, K., Dill, J. (2013). Hyperspectral images lossless compression using the 3D binary EZW algorithm. Image Processing: Algorithms and Systems XI. https://doi.org/10.1117/12.2002820
14. Li, C., Guo, K. (2014). Lossless Compression of Hyperspectral Images Using Three-Stage Prediction with Adaptive Search Threshold. International Journal of Signal Processing, Image Processing and Pattern Recognition, 7 (3), 305–316. https://doi.org/10.14257/ijsip.2014.7.3.25
15. Gashnikov, M., Glumov, N. (2016). Onboard processing of hyperspectral data in the remote sensing systems based on hierarchical compression. Computer Optics, 40 (4), 543–551. https://doi.org/10.18287/2412-6179-2016-40-4-543-551
16. Gashnikov, M. (2017). Minimizing the entropy of post-interpolation residuals for image compression based on hierarchical grid interpolation. Computer Optics, 41 (2), 266–275. https://doi.org/10.18287/2412-6179-2017-41-2-266-275

17. Sarinova, A., Zamyatin, A., Cabral, P. (2015). Lossless compression of hyperspectral images with pre-byte processing and intra-bands correlation. DYNA, 82 (190), 166–172. https://doi.org/10.15446/dyna.v82n190.43723
18. Zamjatin, A. V., Sarinova, A. Zh. (2017). Algorithm for compressing hyperspectral aerospace images using mathematical processing and taking into account interband correlation. Materials of the IV International Scientific Conference "Regional Problems of Earth Remote Sensing", 157–160.
19. Dubey, V. A., Dubey, R. (2013). A New Set Partitioning in Hierarchical (SPIHT) Algorithm and Analysis with Wavelet Filters. International Journal of Innovative Technology and Exploring Engineering, 3 (3), 125–128. Available at: https://www.ijitee.org/wp-content/uploads/papers/v3i3/C1132083313.pdf
20. Kiely, A., Klimesh, M., Xie, H., Aranki, N. (2006). ICER-3D: A Progressive Wavelet-Based Compressor for Hyperspectral Images. The Interplanetary Network Progress Report.
21. Sindhuja, N. M., Arumugam, A. S. (2013). SPIHT based compression of hyper spectral images. International Journal of Advanced Research in Electrical, Electronics and Instrumentation Engineering, 2 (10), 4933–4938. Available at: https://www.ijareeie.com/upload/2013/october/26SPIHT.pdf
22. Penna, B., Tillo, T., Magli, E., Olmo, G. (2006). Progressive 3-D Coding of Hyperspectral Images Based on JPEG 2000. IEEE Geoscience and Remote Sensing Letters, 3 (1), 125–129. https://doi.org/10.1109/lgrs.2005.859942
23. Sujithra, D. S., Manickam, T., Sudheer, D. S. (2013). Compression of hyperspectral image using discrete wavelet transform and Walsh Hadamard transform. International journal of advanced research in electronics and communication engineering (IJARECE), 2 (3), 314–319.
24. Pizzolante, R., Carpentieri, B. (2013). On the Compression of Hyperspectral Data. IT CoNvergence PRActice (INPRA), 1 (4), 24–38. Available at: https://isyou.info/inpra/papers/inpra-v1n4-02.pdf
25. Christophe, E. (2011). Hyperspectral Data Compression Tradeoff. Optical Remote Sensing, 9–29. https://doi.org/10.1007/978-3-642-14212-3_2